A Complete Thermal Analysis of a Funnel-Type Mold Used in High-Speed Thin Slab Continuous Casting Through Three-Dimensional Inverse Heat Conduction Problem

Ce Liang, Haihui Zhang, and Wanlin Wang

Abstract Accurate quantification of heat flux during high-speed thin slab continuous casting is essential for the design and development of the products as well as operation and quality control of the casting process. A novel method for the estimation of the funnel-type mold based on the measured responding temperatures from two surfaces of thermocouples that embedded inside the funnel mold during continuous casting has been developed. The method includes a Three-Dimensional Inverse transient Heat Conduction Problem (3D-IHCP) model that is solved by the conjugate gradient method. The results indicated that the heat fluxes and temperatures across funnel mold hot surface calculated by 3D-IHCP show the same variation tendency as those calculated by 2D-IHCP. Nevertheless, the heat fluxes calculated by 3D-IHCP are larger than those calculated by 2D-IHCP for the locations below the meniscus at the funnel and transition region, but are closed to those calculated by 2D-IHCP for the other positions due to the inclined wall of the funnel-type mold and the convex mold curvature.

Keywords Thin slab casting · Funnel mold · Heat flux · Inverse problem · Three-dimensional

C. Liang · W. Wang (✉)
School of Metallurgy and Environment, Central South University, Changsha 410083, China
e-mail: wanlin.wang@gmail.com

National Center for International Research of Clean Metallurgy, Central South University, Changsha 410083, China

H. Zhang
Faculty of Materials Metallurgy and Chemistry, Jiangxi University of Science and Technology, Ganzhou 341000, China

Introduction

The development of processes for near-net-shape-casting is one of the important recent trends to reduce the cost and increase the productivity [1]. Compact strip production (CSP), one kind of thin slab and hot direct rolling technology, could produce thin slabs closer to the dimensions of the final product [2]. However, the special funnel-type mold shape and high casting speed condition of thin slab casting always lead to a high average heat flux, and especially, a much higher local heat flux near the meniscus, which give rise to differential thermal expansion that in turn leads to severe slab defects and mold distortion [3]. Consequently, the local transient heat flux across the funnel-type mold must be carefully monitored and controlled.

Accurate heat flux cannot be directly measured or calculated due to inherent limitations in an actual industrial set-up. To alleviate such problems, the inverse heat conduction problem (IHCP) is being employed in recent times which utilize the temperature data measured inside the mold using sensors fixed at some accessible locations. The first step in IHTP is to guess the boundary heat flux and calculate the temperature at the specified points where the temperature can be measured. The next step is to minimize the objective function formed by the difference between measured and estimated temperatures. Udayraj et al. [4] estimated the one-dimensional variation of heat flux along the casting direction of a square cross-sectional billet mold using only limited temperature measurements. Yao et al. [5] developed a similar two-dimensional inverse transient heat conduction problem model to investigate the mold heat flux. Nevertheless, the heat flux variation of a funnel-type mold with a very high aspect ratio across length and width is much more complex compared to the conventional continuous casting because of turbulent flow of liquid metal and larger mechanical force between the strand and the mold surface which in turn results in the non-uniform thermal behavior of the mold. Thus, a three-dimensional unsteady-state heat transfer inverse problem model could be a better option to describe the heat transfer mechanism in the funnel-type mold.

Therefore, the objective of this work is to further develop a Three-Dimensional Inverse transient Heat Conduction Problem (3D-IHCP) model with improved CGM algorithm and Finite Element Method (FEM) for the estimation of heat flux in the funnel-type mold, based on above 1D-IHCP and 2D-IHCP [6, 7]. The reason for CGM algorithm to be used here to solve the 3D-IHCP is because it is one of the most effective techniques for the inverse problem and is very convenient to be extended from one case to other similar cases. The CGM algorithm has been successfully applied in many studies [4, 8, 9].

Mathematic Model

Direct Problem Description

The present problem deals with the prediction of the unknown boundary heat flux of a funnel mold which is in direct contact with the liquid steel during thin slab casting process. Figure 1 shows the cross section of the funnel mold simulator system used in this study for the investigation of transient heat flux near the meniscus. It contains a domain **ABCD** which is a funnel-type hexahedron with a horizontal length of 60, 8 mm in width, and 20 mm in height. A half slice of the **ABCD** is formed by cutting it symmetrically across its length, as shown in Fig. 2. Because of this symmetry, the half part is considered as a problem domain Ω of which has six boundaries of $\Gamma_1, \Gamma_2, \Gamma_3, \Gamma_4, \Gamma_5$ (symmetry plane) and Γ_6 (in Fig. 2). The K type thermocouples embedded in the mold wall are divided into two groups by two surfaces with 3 and 8 mm away from the mold hot surface. The TCs on the first surface should be located as close as possible to the boundary Γ_1 to catch the variations of temperatures and to be used in the minimization process of the objective function. The TCs on the second surface are located in Γ_6 which could provide the temperature boundary condition to have a better reconstruction of the transient local heat flux in the funnel mold during continuous casting. By assuming the mold, heat transfer phenomenon is a three-dimensional transient-state problem along the casting direction, longitudinal and transverse directions. The heat transfer within the mold is assumed to be governed by Fourier partial differential equations. The direct problem here is to determine the temperature field of calculated domain $\Omega = \{(x, y, z)|0 < x < 8, 0 < y < 30, 0 < z < 20\}$, where the heat fluxes $q(\Gamma_1, t)$, $q(\Gamma_2, t)$, $q(\Gamma_3, t)$, and $q(\Gamma_4, t)$ are given and known. The mathematic formula of this problem is given by,

$$\rho c \frac{\partial T}{\partial t} = \frac{\partial}{\partial x}\left(\lambda \frac{\partial T}{\partial x}\right) + \frac{\partial}{\partial y}\left(\lambda \frac{\partial T}{\partial y}\right) + \frac{\partial}{\partial z}\left(\lambda \frac{\partial T}{\partial z}\right), \text{ in } \Omega, t \in [0, t_f] \tag{1a}$$

$$-\lambda \frac{\partial T}{\partial \mathbf{n}}\bigg|_{\Gamma_{1,2,3,4}} = \mathbf{q}, \text{ to be estimated} \tag{1b}$$

$$-\lambda \frac{\partial T}{\partial \mathbf{n}}\bigg|_{\Gamma_5} = 0, \text{ symmetry} \tag{1c}$$

$$T(\Gamma_6, t) = f(t), \text{ on } \Gamma_6, \text{ measured} \tag{1d}$$

$$T(x, y, z, 0) = T_{ini} \tag{1e}$$

where T denotes the temperature defined on an observation time interval $[0, t_f]$ and on a 3D funnel-type domain Ω. $\mathbf{q}$ is the time- and spatial-dependent heat fluxes on different boundaries $\Gamma_1, \Gamma_2, \Gamma_3$, and Γ_4. At the symmetry plane Γ_5, corresponding symmetry boundary conditions are applied. $\mathbf{n}$ is outer normal of boundary, and $f(t)$

Fig. 1 Schematic diagrams of the funnel mold (cross section)
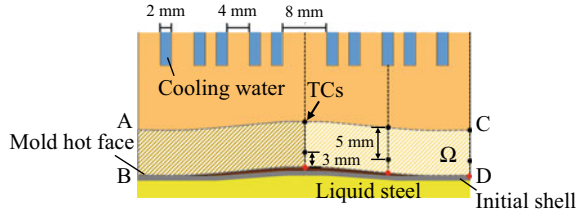
Fig. 2 Computational domain Ω for 3D-IHCP with boundary conditions
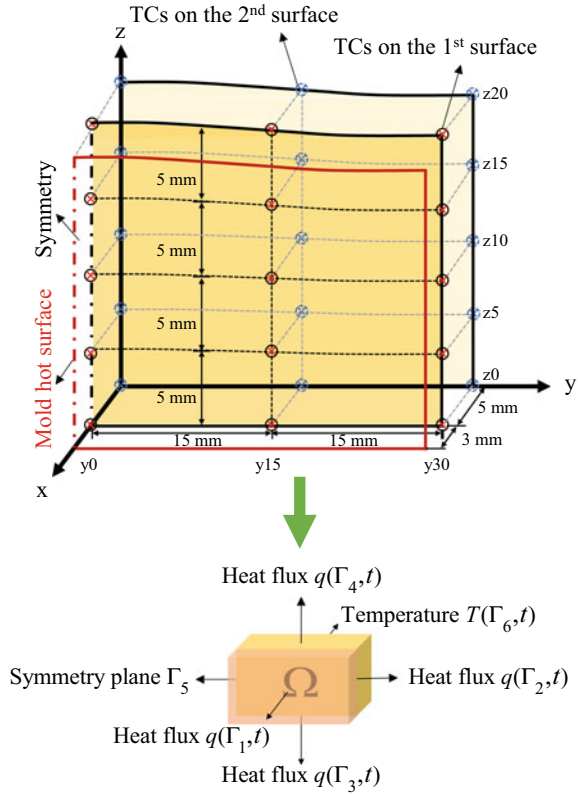
is the temperature boundary condition that is obtained by the way of interpolation from temperatures measured by thermocouples on Γ_6. ρ, c, and λ denote the density, the heat capacity, and the thermal conductivity, respectively. The direct problem of calculating the temperatures of the computational domain Ω at various locations using the boundary conditions is achieved using the above equations (Eq. 3).

Inverse Problem Description

The inverse problem deals with the prediction of the boundary heat flux from the temperature measured by thermocouples inside the funnel mold, so that the sum of the square of the deviation between the calculated temperatures and the measured temperatures would be minimum. Therefore, the solution of inverse problem is based on the minimization of the least square norm,

$$s(q) = \|\mathbf{Y}_m - \mathbf{T}_c(q)\|^2 \tag{2}$$

is considered as the objective functional. $\|\cdot\|$ denotes the norm in the set of L^2 functions. Where Y_m and T_c are the measured and calculated temperatures at the measurement locations, respectively, and q represents the heat fluxes at boundaries Γ_1, Γ_2, Γ_3, and Γ_4.

Conjugate Gradient Method for Minimization

The CGM minimizes the objective function (Eq. 2) at each iterative calculation by choosing the new guess heat flux $\hat{\mathbf{q}}^{k+1}$ on the boundary according to

$$\hat{\mathbf{q}}^{k+1} = \hat{\mathbf{q}}^k - \beta^k d^k \tag{3}$$

With $\hat{\mathbf{q}}^0 = 0$, β^k is the search step in each iteration k. The conjugate search direction d^k is updated by

$$d^k = \nabla J^k + \gamma^k d^{k-1}, \ k \geq 2 \tag{4a}$$

$$d^k = \nabla J^k, \ k = 1 \tag{4b}$$

where the gradient ∇J^k is determined by

$$\nabla J^k = \Psi^k \tag{5}$$

and Ψ^k is obtained from adjoint problem which corresponds to

$$-\rho c \frac{\partial \Psi^k}{\partial t} = \nabla \cdot (\lambda \nabla \Psi^k)$$

$$+ 2 \sum_{m=1}^{M} \{Y_m - T_c(q)\} \delta(x - x_m) \delta(y - y_m) \delta(z - z_m), \ \text{in } \Omega, t \in [0, \, t_f] \tag{6a}$$

$$-\lambda \frac{\partial \Psi^k}{\partial \mathbf{n}}\Big|_{\Gamma_{1,2,3,4,5}} = 0 \tag{6b}$$

$$\Psi^k(\Gamma_6, t) = 0, \text{ on } \Gamma_6 \tag{6c}$$

$$\Psi^k(x, y, z, 0) = 0 \tag{6d}$$

where $\delta(x_m, y_m, z_m)$ is the Dirac delta function, the (x_m, y_m, z_m) represents the locations of thermocouples, and M is the total number of thermocouples.

The conjugate coefficient γ^k in Eqs. (4a, 4b) is obtained from

$$\gamma^k = \frac{\int_0^{t_f} \int_\Gamma (\nabla J^k)^2 dx dt}{\int_0^{t_f} \int_\Gamma (\nabla J^{k-1})^2 dx dt}, \ k \geq 2 \tag{7a}$$

$$\gamma^k = 0, \ k = 1 \tag{7b}$$

In each iteration, the search step β^k in Eq. 3 is determined by solving the sensitivity problem. The sensitivity problem takes the form

$$-\rho c \frac{\partial S^k}{\partial t} = \nabla \cdot (\lambda \nabla S^k), \text{ in } \Omega, t \in [0, t_f] \tag{8a}$$

$$-\lambda \frac{\partial S^k}{\partial \mathbf{n}}\Big|_{\Gamma_{1,2,3,4}} = p^k, \ p^k\big|_{\Gamma_{1,2,3,4}} = \nabla J^k\big|_{\Gamma_{1,2,3,4}} \tag{8b}$$

$$S^k(x, y, z, 0) = 0 \tag{8c}$$

$$J^k(\Gamma_6, t) = 0, \text{ on } \Gamma_6 \tag{8d}$$

$$J^k(x, y, z, 0) = 0 \tag{8e}$$

and β^k is determined by

$$\beta^k = \frac{\int_0^{t_f} \int_\Gamma (T_c - Y_m) S^k dx dt}{\int_0^{t_f} \int_\Gamma (S^k)^2 dx dt} \tag{9}$$

After each iteration, the value of estimated $\hat{\mathbf{q}}$ is updated and the convergence of the objective function $S(q)$ to an acceptable value is checked. The procedure continues until either the intended convergence criteria or the maximum number of iterations have been reached or not. The discrepancy principle based on previous studies is used to choose ε where the residuals between the calculated temperatures and the measured ones are of the same order of the temperature measurement errors. Then,

the temperature residuals are approximated by

$$\|\mathbf{Y}_m - \mathbf{T}_c(q)\|^2 \approx M\varepsilon^2 \qquad (10)$$

Solution Procedure

The geometry of the mold computational domain is developed using SOLIDWORKS software, and this geometry is imported to COMSOL Multiphysics software. Hexahedral mesh with 4640 mesh elements is generated using COMSOL sweeping algorithms which caters to the whole volume of the problem domain including the funnel zone by suitably adjusting the meshing parameters. The unknown boundary conditions are assumed as zero first, and subsequently, the boundary conditions are applied as discussed in Eq. 3. The discretization of the governing partial differential equations is done using the Finite Element Method (FEM). An iterative procedure is adopted under the control of MATLAB software for convergence of the direct problem. The temperatures within the computational domain are obtained by solving direct problem (Eqs. 1a–1e) using COMSOL. A suitable technique is coded for solving the inverse problem as discussed in Eq. 2 which is developed using MATLAB. As the stopping criterion is fulfilled or the maximum number of iterations 200 is reached, the iterative procedure would be terminated by MATLAB. The conjugate gradient method is coded using MATLAB and the gradient ∇J^k in the adjoint problem and the search step β^k in the sensitivity problem are calculated using COMSOL.

Validation Test

Methodology of Validation

In this section, a numeric benchmark is designed to provide simulated experiment data for the verification of the 3D-IHCP model. As shown in Fig. 2, the test problem domain is a funnel-type hexahedron with a horizontal length of 30, 8 mm in width, and 20 mm in height. The material of the computational area is copper and the initial temperature is 288 K. The boundaries Γ_2, Γ_3, Γ_4, and Γ_5 are insulted, while Γ_6 is water cooling with convection heat transfer coefficient of 1×10^4 W/(m^2 K). The temperature of cooling water is also 288 K. The test heat fluxes are applied on Γ_1 to investigate the accuracy of the 3D-IHCP model. The simulated heat flux $q(y, z, t)$ imposed on the front surface Γ_1 is of triangular type in space and explicitly defined by

$$q(\Gamma_1, t) = \begin{cases} 0, & 0 \le t < 1 \\ 2 \times 10^6 \left(\frac{50-(y+z)}{50} \times \frac{(t-1)}{1.5} \right), & 1 \le t < 2.5 \\ 2 \times 10^6 \left(\frac{50-(y+z)}{50} \times \frac{(4-t)}{1.5} \right), & 2.5 \le t < 4 \\ 0, & 4 \le t \le 5 \end{cases} \qquad (11)$$

For the numerical simulation, the noise-free temperature Y is obtained by solving direct problem. Fifteen virtual response thermocouples on the first surface are located 3 mm away from the Γ_1 to provide the temperature for minimizing the objective function of inverse calculation, while the other fifteen virtual thermocouples on the second surface are 8 mm away from the Γ_1 to provide the temperature boundary condition on Γ_6. The test problem domain is discretized into hexahedral mesh with approximately a size of 1 mm $\times$ 1 mm $\times$ 1 mm and 0.01 s time-step is set to run the direct problem test using COMSOL. Meanwhile, the 'temperature measurement' is taken every 0.1 s. The measured simulated temperatures are delivered to the 3D-IHCP model for the estimation of the heat flux on the boundary. Finally, the Gaussian noise signals $\omega\sigma$ are added to the simulated temperatures to mimic the thermocouple measurement errors for the testing of the anti-noise ability of the inverse problem model. In this study, $\sigma = 0, 0.1\% Y_{\max}, 0.2\% Y_{\max}$ is applied, and ω is a random variable and will be within -2.576 to 2.576 for the 99 pct confidence bounds. Additionally, L2 Euclidean norm between the pre-set heat flux and the recovered heat flux, $\|\mathbf{q} - \hat{\mathbf{q}}\|$, is used to evaluate the accuracy of reconstruction results, where the large of L2 norm implies the poor reconstruction of heat flux by the inverse problem algorithm. To be more precise, the e_{RMS} error is defined based on the L2 Euclidean errors' norm to analyze the accuracy of the inverse problem,

$$e_{RMS} = \frac{\|\mathbf{q} - \hat{\mathbf{q}}\|}{\|\mathbf{q}\|} \times 100\% \qquad (12)$$

Validation Results

Figure 3 shows the comparison of the estimated heat flux calculated by 3D-IHCP with the exact value, where the heat fluxes at five points (8, 0, 0), (8, 30, 0), (7.8, 15, 10), (8, 30, 20), and (6.5, 0, 20) mm are extracted. It was found that the heat fluxes calculated by 3D-IHCP model agree well with the exact values. The calculated heat fluxes also match with the exact values when the measurement errors are involved in the 'measured' simulated temperatures. This suggested that the 3D-IHCP shows less sensitivity to measurement errors. As the measurement error σ increases from $0.1\% Y_{\max}$ to $0.2\% Y_{\max}$, the fluctuations of the recovered heat fluxes also increase indicating that the dependency of the inverse calculation accuracy is also influenced by the standard deviation of noise.
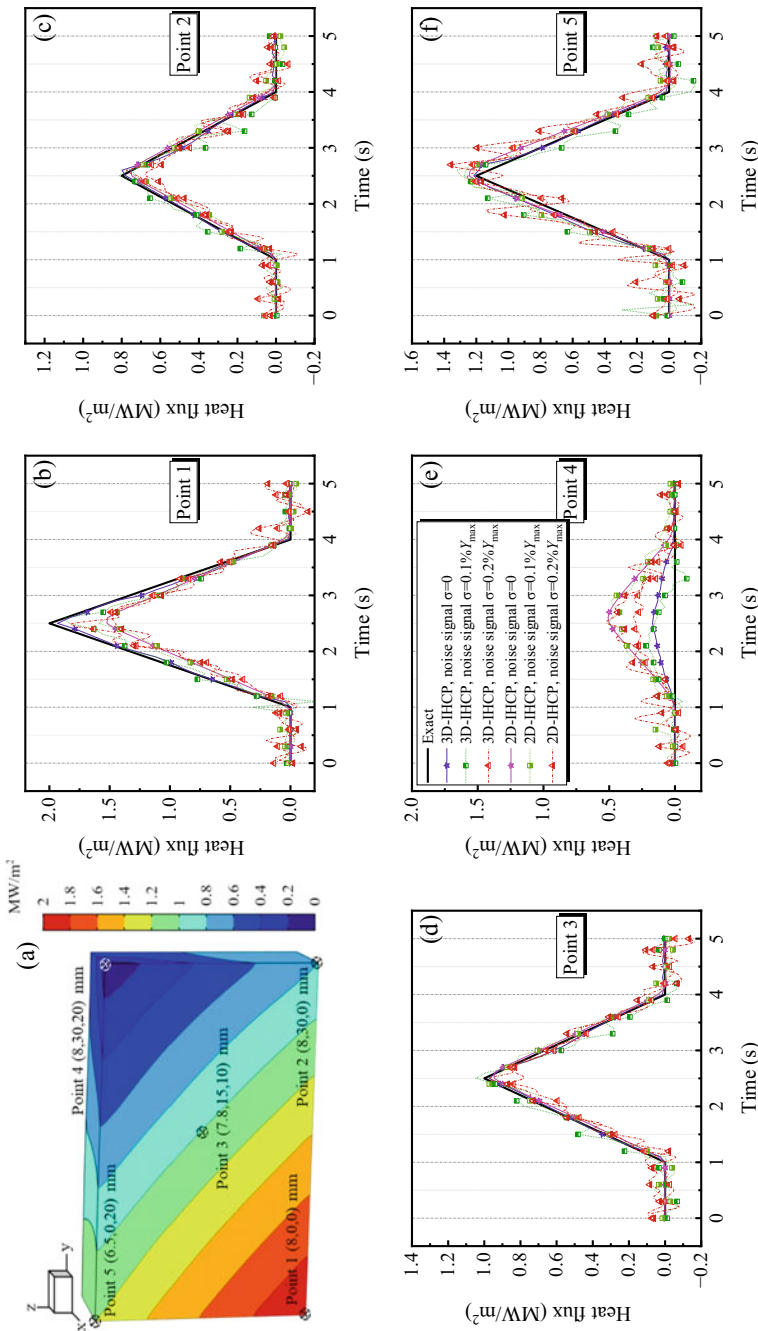
Fig. 3 Comparison of the exact mold hot surface heat flux with the calculated heat flux by 3D-IHCP and 2D-IHCP: **a** calculated heat flux contour calculated by 3D-IHCP, **b** heat flux at point 1 (8, 0, 0) mm, **c** heat flux at point 2 (8, 30, 0) mm, **d** heat flux at point 3 (7.8, 15, 10) mm, **e** heat flux at point 4 (8, 30, 20) mm, **f** heat flux at point 5 (6.5, 0, 20) mm

However, the heat fluxes calculated by 3D-IHCP at point 4 (8, 30, 20) mm show deviations with the exact value as shown in Fig. 3e. The difference could attribute to the arrangement of thermocouples in the computed domain. Generally, the more measurements taken and closer to the boundary, the more precise of the recovered results would be.

Conclusion

A robust 3D-IHCP model is developed for the estimation of the space- and time-dependent heat flux across the funnel mold used in the thin slab continuous casting. The method is based on the measured temperatures from two surfaces of thermo-couples embedded in the funnel mold wall. The main conclusions are described as follows:

1. The 3D-IHCP could be successfully applied to the calculation of the heat flux of the funnel mold hot surface for continuous casting.
2. The results of 3D-IHCP could provide more precise heat flux calculation method than 2D-IHCP, especially for the funnel and transition region of the funnel mold.

References

1. Vakhrushev A, Wu M, Ludwig A, Tang Y, Hackl G, Nitzl G (2014) Numerical investigation of shell formation in thin slab casting of funnel-type mold. Metall Mater Trans B 45:1024–1037
2. Nam H, Park HS, Yoon JK (2000) Numerical analysis of fluid flow and heat transfer in the funnel type mold of a thin slab caster. ISIJ Int 40:886–892
3. Vaka AS, Ganguly S, Talukdar P (2021) Novel inverse heat transfer methodology for estimation of unknown interfacial heat flux of a continuous casting mould: a complete three-dimensional thermal analysis of an industrial slab mold. Int J Therm Sci 160:106648
4. Udayraj S, Chakraborty S, Ganguly EZ, Chacko SKA, Talukdar P (2017) Estimation of surface heat flux in continuous casting mold with limited measurement of temperature. Int J Therm Sci 118:435–447
5. Wang X, Tang L, Zang X, Yao M (2012) Mold transient heat transfer behavior based on measurement and inverse analysis of slab continuous casting. J Mater Process Technol 212:1811–1818
6. Zhang H, Wang W, Zhou L (2015) Calculation of heat flux across the hot surface of continuous casting mold through two-dimensional inverse heat conduction problem. Metall Mater Trans B 46:2137–2152
7. Wang S, Ni R (2019) Solving of two-dimensional unsteady-state heat-transfer inverse problem using finite difference method and model prediction control method. Complexity
8. Parwani AK, Talukdar P, Subbarao PMV (2015) Estimation of boundary heat flux using experimental temperature data in turbulent forced convection flow. Heat Mass Transf 51:411–421
9. Amin MR, Gawas NL (2003) Conjugate heat transfer and effects of interfacial heat flux during the solidification process of continuous castings. J Heat Transfer 125:339–348